

## **Supporting Information**

### **An exceptionally stable functionalized metal-organic framework for lithium storage**

**Yichao Lin, Qiuju Zhang, Chongchong Zhao, Huailong Li, Chunlong Kong,\* Cai Shen\*  
and Liang Chen\***

Institute of Materials Technology and Engineering, Chinese Academy of Sciences, Ningbo,  
Zhejiang 315201, China

\*e-mail: chenliang@nimte.ac.cn, shencai@nimte.ac.cn, kongchl@nimte.ac.cn

### **Table of Contents**

- 1. Experimental details**
- 2. Computational details**
- 3. Additional Figures**

## 1. Experimental Details

### Materials and methods

Powder X-ray Diffraction (XRD) were collected on a Bruker AXS D8 Advance diffractometer using CuK $\alpha$  ( $\lambda = 1.5406 \text{ \AA}$ ) radiation at a voltage of 40 kV and 40 Ma, and the powder diffraction pattern was scanned over the angular range of 5-40° (2 $\theta$ ) with a step size of 0.02°. Scanning electron microscopy images were taken on Hitachi S-4800. Transmission electron microscopy images were examined on Tecnai F20. X-ray photoelectron spectroscopy (XPS) were measured on a Kratos AXIS ULTRA<sup>DLD</sup> instrument with a monochromic Al-K $\alpha$  X-ray source ( $h\nu = 1486.6 \text{ eV}$ ). Infrared spectra (IR) were recorded on KBr/BMOF pellets in a Thermo model Nicolet 6700 spectrometer. Thermogravimetric (TG) analyses were performed under N<sub>2</sub> and air on a Mettler Toledo (model Pyris Diamond TG/DTA), with a heating rate of 5 °C min<sup>-1</sup>. Nitrogen adsorption/desorption isotherm was measured on ASAP 2020M apparatus at 77.3 K. Solvents, reagents and chemicals were purchased from Aldrich and Alfa. All the solvents, reagents and chemicals were used as purchased unless stated otherwise. Room-temperature <sup>1</sup>H $\rightarrow$ <sup>13</sup>C CP-MAS NMR experiments were performed with a double tuned 4.0 mm probe on a Bruker Avance III 400 spectrometer in a magnetic field strength of 9.4 T at Larmor frequencies of 400.13 MHz (<sup>1</sup>H) and 100.66 MHz (<sup>13</sup>C). Powdered samples were packed inside zirconia MAS rotors and spun at 14 kHz. The Hartmann Hahn condition was determined on a sample of adamantane. TPPM <sup>1</sup>H decoupling was applied during the acquisition. Recycle delays and contact time were optimized experimentally on the samples, which were set at 1 s and 3 ms.

### Electrode Fabrication and Electrochemical Measurement

The Electrochemical measurements were carried out using 2032-type coin cells system with metallic lithium as the counter electrode. The working electrodes were prepared by coating a mixture of 70 wt% BMOF, 20 wt% conductive carbon black(super P), and 10 wt% polyvinylidene fluoride(PVDF) onto a copper foil. The cell assembly was operated in an argon-filled glove box with Oxygen and moisture concentrations below 0.1 ppm. The electrolyte solution consisted of 1 M LiPF<sub>6</sub> in a

solution of fluoroethylene carbonate(FEC), dimethyl carbonate(DMC), and ethyl methyl carbonate(EMC) with the volume ratio of 1:1:1. Celgard 2400 polypropylene was used as separator. Charge/discharge measurements were carried out galvanostatically at various current densities(20-400 mA/g) over a voltage range of 0.01 – 3.0 V(v.s. Li/Li<sup>+</sup>) by using a battery test system(LAND model, CT2001A, Wuhan RAMBO testing equipment, Co. Ltd.) at 30°C.

### **Synthesis of bifunctional metal-organic framework (BMOF)**

To a solution of 2-aminobenzimidazole (abIM) (120 mg, 0.9 mmol), imidazole (IM) (184 mg, 2.7 mmol), and zinc nitrate hexahydrate (268 mg, 0.9 mmol) in anhydrous N, N-dimethylformamide (DMF) (30ml), and the mixture was stirred at room temperature for 1 hour. Then, the mixture was heated at 130 °C for 72 h under autogenous pressure. The light yellow crystals were observed in the Teflon vessel and collected, then washed with DMF at room temperature for 2~3 times every other day to remove the most unreacted reactants, and then the products were further washed with alcohol at room temperature for 24 h to remove the solvent DMF effectively. Finally, the products were first dried at 80 °C for 3 hour under vacuum, then at 220 °C for 12 h to remove the alcohol and the DMF in the pores of the products.

### **Single-crystal X-ray crystallography**

Single crystal X-ray diffraction analysis of the crystal was collected on a Bruker SMART APEX CCD diffractometer with graphite-monochromated Mo-K $\alpha$  ( $\lambda$  = 0.71073 Å) using the SMART and SAINT programs. The structures were solved by direct methods and refined on F<sup>2</sup> by full-matrix least-squares methods with SHELXTL version 5.1.

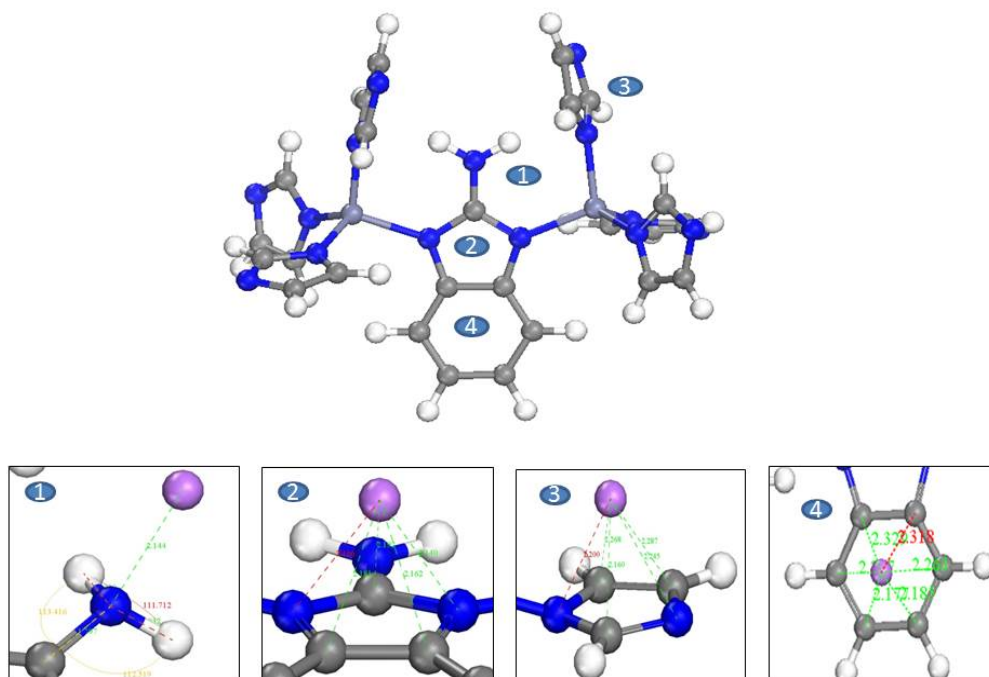
### **PMMA/BMOF composite preparation**

0.8 g BMOF (evacuated under 220 °C for 12 hours) was added step by step into a 25 ml tetrahydrofuran solution containing 0.2 g PMMA under stirring. The resulting mixture was stirred and dried at room temperature.

## 2. Computational details

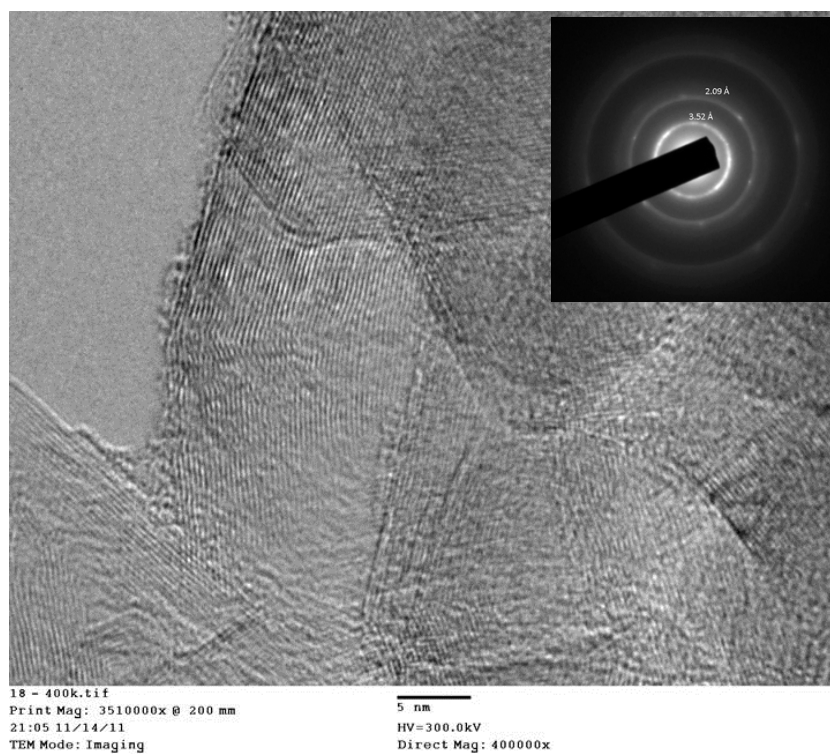
All the calculations were performed by the density functional theory using the Vienna ab initio simulation package (VASP version 5.2.11). The electron-ion interactions were treated by all-electron projector augmented wave (PAW) approximation. Electronic exchange-correlation energies were performed by Perdew, Burke and Enzer (PBE) functional within the spin-polarized generalized gradient approximation (GGA). The cutoff energy was set to 350 eV for the plane wave basis set. All atoms were relaxed with the convergence to 0.03 eV/Å ions for forces and  $10^{-4}$  eV/Å for total energy. Fragment BMOF are constructed in a cubic box with  $a=20$  Å. The Monkhorst-Pack mesh of  $2 \times 2 \times 2$  was employed. The binding energy of Li atom adsorbed on BMOF fragment is defined as:  $E_{ab} = E_{Li/BMOF} - E_{BMOF} - E_{Li}$ .

### 3. Additional Figures



Binding site	$E_{ab}$	$d(\text{Li-M})$
		$\text{M}=\text{NH}_2, \text{C}_6\text{H}_4, \text{C}_3\text{N}_2$
① Li-NH <sub>2</sub>	-2.300eV	2.144Å
② Li-C <sub>3</sub> N <sub>2</sub> -NH <sub>2</sub>	-2.000eV	1.832Å
③ Li- C <sub>3</sub> N <sub>2</sub> -Zn	-3.133eV	1.859Å
④ Li-C <sub>6</sub> H <sub>4</sub>	-3.653eV	1.826Å

Fig. S1. The binding sites for Li storage and the corresponding binding energy.



Plane spacings are about 3.5 Å.

Fig. S2. TEM images of the as-prepared BMOF.

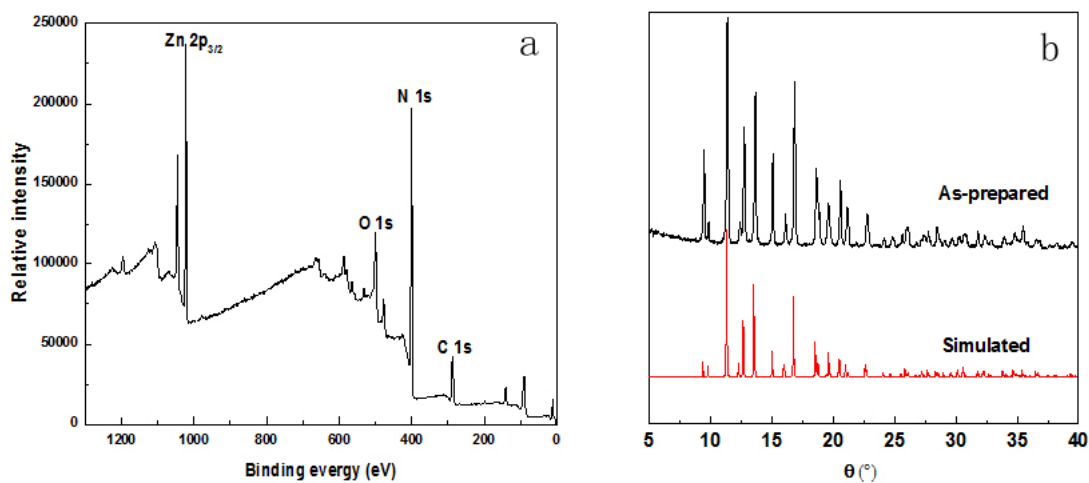


Fig. S3. (a) X-ray photoelectron spectroscopy of the as-prepared BMOF. (b) Powder and simulated XRD patterns of the crystal BMOF.

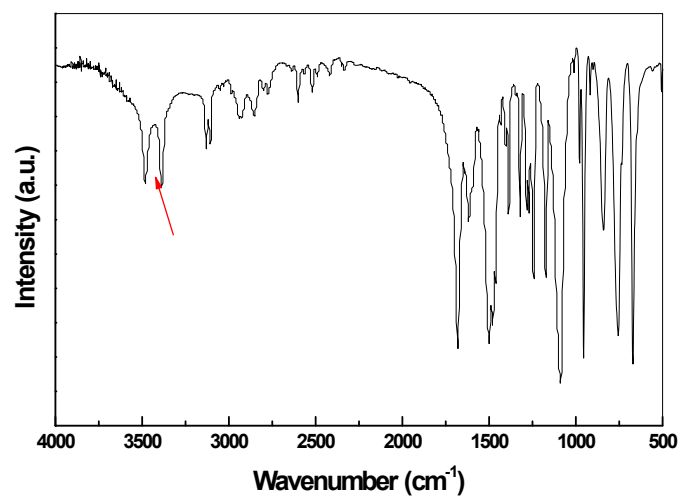


Fig. S4. IR spectra of the BMOF.

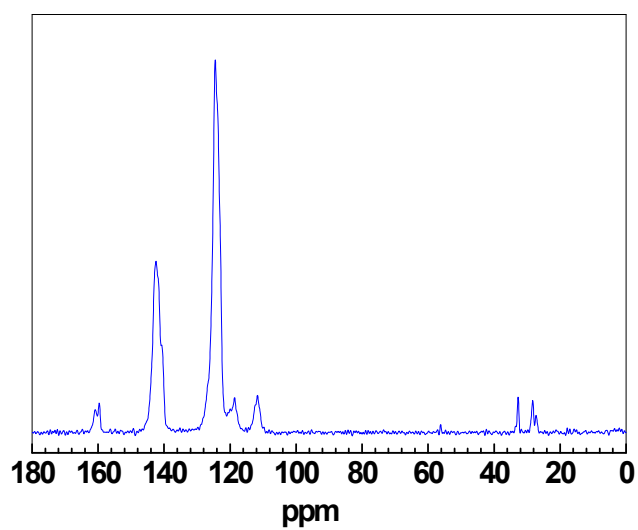


Fig. S5. Solid-state <sup>13</sup>C NMR spectra of the BMOF.

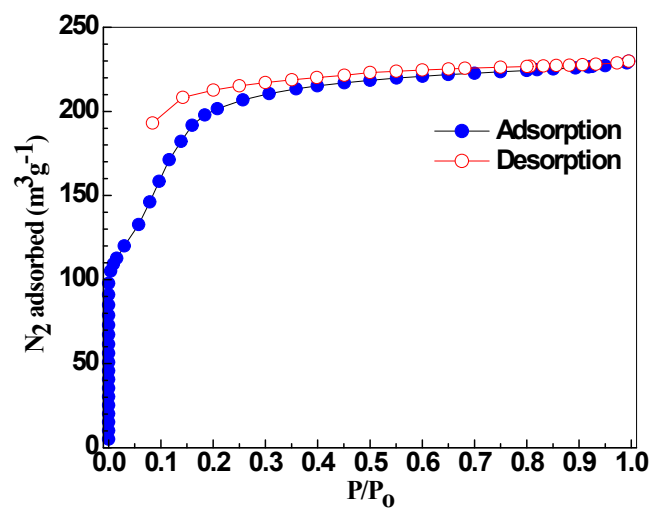


Fig. S6. N<sub>2</sub> adsorption-desorption isotherms of BMOF at 77.3 K. Key: ○ desorption isotherm, ● adsorption isotherm.

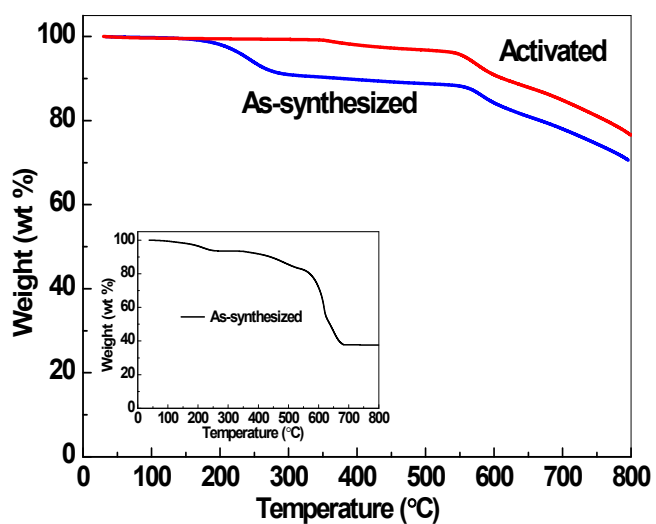


Fig. S7. The TG analysis traces of as-synthesized, evacuated (activated) samples of the BMOF in nitrogen. The inset is TG analysis traces of as-synthesized BMOF in air.



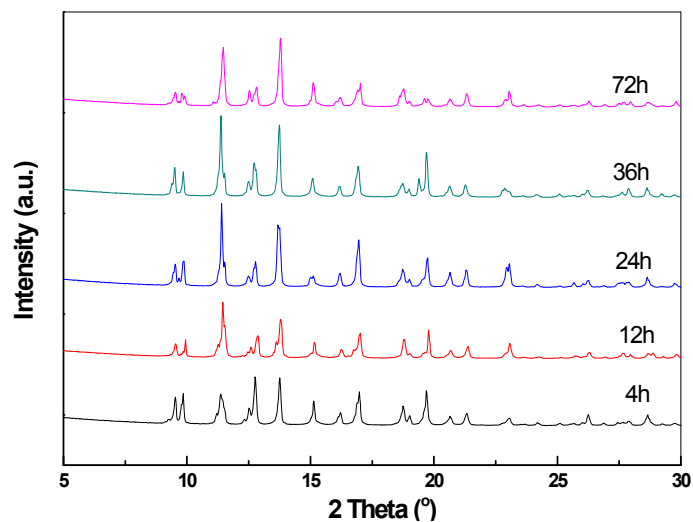


Fig. S8. The PXRD patterns of BOMF after heated at 200 °C in air for different periods of time.

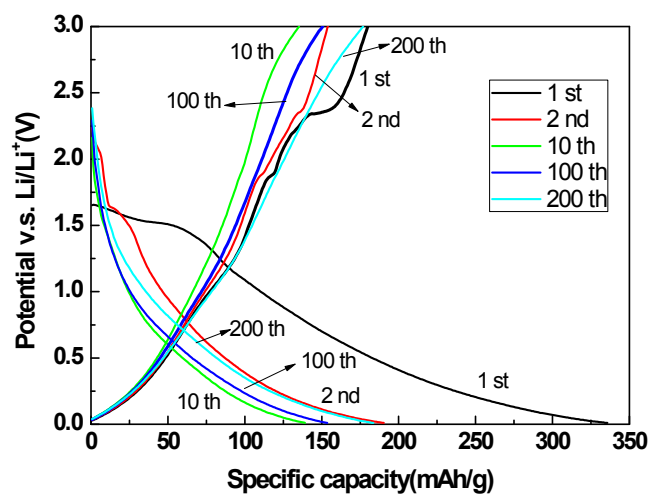


Fig. S9. Discharge-charge profiles of the electrodes made with the BMOF. The discharge/charge process was carried out under constant current density of 100 mA/g.

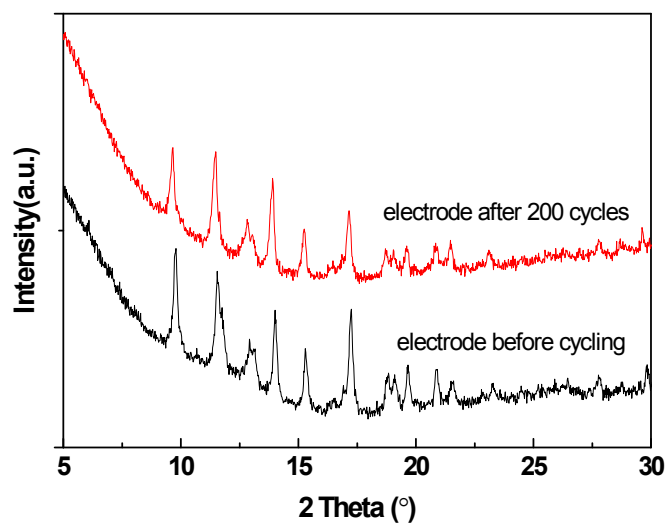


Fig. S10. XRD patterns of BMOF-based electrodes before and after cycling.

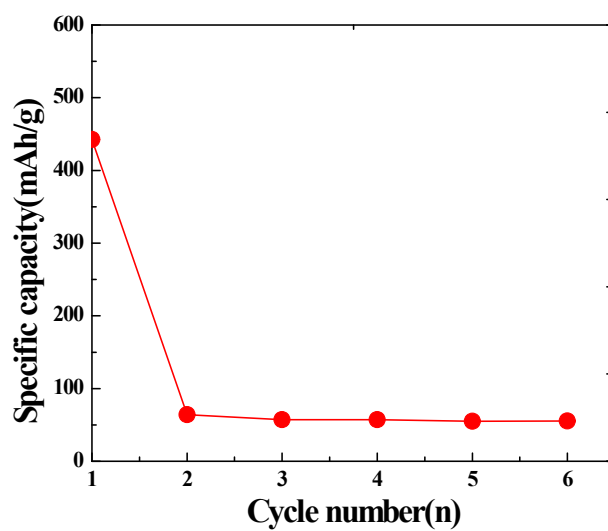


Fig. S11. Cycling performance and Coulombic efficiency of the electrodes made with abIM at 50 mA/g.

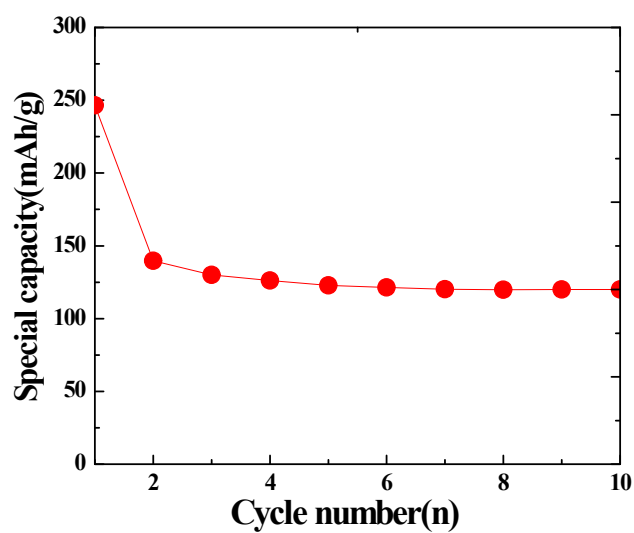


Fig. S12. Cycling performance and Coulombic efficiency of the electrodes made with PMMA/BMOF (the data is based on the weight of BMOF) at 50 mA/g.